

UC Berkeley

UC Berkeley Previously Published Works

Title

Spectroscopic search for optical emission lines from dark matter decay

Permalink

<https://escholarship.org/uc/item/72k887mx>

Journal

Physical Review D, 110(10)

ISSN

2470-0010

Authors

Wang, Hanyue

Eisenstein, Daniel J

Aguilar, Jessica Nicole

et al.

Publication Date

2024-11-15

DOI

[10.1103/physrevd.110.103007](https://doi.org/10.1103/physrevd.110.103007)

Copyright Information

This work is made available under the terms of a Creative Commons Attribution License, available at <https://creativecommons.org/licenses/by/4.0/>

Peer reviewed

A Spectroscopic Search for Optical Emission Lines from Dark Matter Decay

Hanyue Wang^{1,2}, Daniel J. Eisenstein^{1,2}, Jessica Nicole Aguilar³, Steven Ahlen⁴, Stephen Bailey³, David Brooks⁵, Todd Claybaugh³, Axel de la Macorra⁶, Peter Doel⁵, Jaime E. Forero-Romero⁷, Anthony Kremin³, Michael E. Levi³, Marc Manera^{8,9}, Ramon Miquel^{9,10}, Claire Poppett³, Mehdi Rezaie¹¹, Graziano Rossi¹², Eusebio Sanchez¹³, Michael Schubnell¹⁴, Gregory Tarlé¹⁴, Benjamin A. Weaver¹⁵, and Zhimin Zhou¹⁶

¹Department of Astronomy, Harvard University, 60 Garden St., Cambridge MA 02138, USA

²Center for Astrophysics | Harvard & Smithsonian, 60 Garden St., Cambridge, MA 02138, USA

³Lawrence Berkeley National Laboratory, 1 Cyclotron Road, Berkeley, CA 94720, USA

⁴Physics Dept., Boston University, 590 Commonwealth Avenue, Boston, MA 02215, USA

⁵Department of Physics & Astronomy, University College London, Gower Street, London, WC1E 6BT, UK

⁶Instituto de Física, Universidad Nacional Autónoma de México, Cd. de México C.P. 04510, México

⁷Departamento de Física, Universidad de los Andes,

Cra. 1 No. 18A-10, Edificio Ip, CP 111711, Bogotá, Colombia

⁸Departament de Física, Serra Húnter, Universitat Autònoma de Barcelona, 08193 Bellaterra (Barcelona), Spain

⁹Institut de Física d'Altes Energies (IFAE), The Barcelona Institute of Science and Technology,

Campus UAB, 08193 Bellaterra Barcelona, Spain

¹⁰Institució Catalana de Recerca i Estudis Avançats,

Passeig de Lluís Companys, 23, 08010 Barcelona, Spain

¹¹Department of Physics, Kansas State University, 116 Cardwell Hall, Manhattan, KS 66506, USA

¹²Department of Physics and Astronomy, Sejong University, Seoul, 143-747, Korea

¹³CIEMAT, Avenida Complutense 40, E-28040 Madrid, Spain

¹⁴Department of Physics, University of Michigan, Ann Arbor, MI 48109, USA

¹⁵NSF's NOIRLab, 950 N. Cherry Ave., Tucson, AZ 85719, USA and

¹⁶National Astronomical Observatories, Chinese Academy of Sciences,

A20 Datun Rd., Chaoyang District, Beijing, 100012, P.R. China

We search for narrow-line optical emission from dark matter decay by stacking dark-sky spectra from the Dark Energy Spectroscopic Instrument (DESI) at the redshift of nearby galaxies from DESI's Bright Galaxy and Luminous Red Galaxy samples. Our search uses regions separated by 5 to 20 arcsecond from the centers of the galaxies, corresponding to an impact parameter of approximately 50 kpc. No unidentified spectral line shows up in the search, and we place a line flux limit of 10^{-19} ergs/s/cm²/arcsec² on emissions in the optical band ($3000 \lesssim \lambda \lesssim 9000 \text{ Å}$), which corresponds to 34 in AB magnitude in a normal broadband detection. This detection limit suggests that the line surface brightness contributed from all dark matter along the line of sight is two orders of magnitude lower than the measured extragalactic background light (EBL), which rules out the possibility that narrow optical-line emission from dark matter decay is a major source of the EBL.

I. INTRODUCTION

Dark matter is an important cornerstone for the standard Λ CDM cosmological model and a main component of current large-scale structure formation history. Cosmological observations have shown that a comparable amount of dark matter is needed at low redshift for galaxy rotation curves, strong gravitational events, and galaxy clustering. Although dark matter is often considered as stable long-lived particles, deviations from this empirical limit would provide critical information about the true nature of dark matter. There are many hypotheses about how particle candidates beyond the Standard Model appear from dark matter decay, for instance, sterile neutrinos [1], gravitinos [2] and axions [3]. These models typically describe how dark matter particles are able to decay through weak coupling with Standard Model particles to radiation, such as two photons [4, 5] or one photon and one other particle (such as Z boson or neutrino) [6]. In certain scenarios, weak coupling with baryons prompts the decay of dark matter into a photon line. One such example is the decay of axion-like parti-

cles, which are known to be unstable and can decay into two photons [7–9]. Additionally, in the neutrino minimal standard model (ν MSM), decay of sterile neutrinos as dark matter candidates emit monoenergetic photons [10].

Dark matter decay properties can be constrained with different processes. [11, 12] study the decay behavior directly from a laboratory setup or detectors and [13] used cosmological N-body simulations to make predictions. There is also an ongoing endeavor to probe with high-energy astronomical observations at the galactic center and dwarf galaxies [14], gamma-ray extragalactic background [15] and in X-Ray [16]. [17] discovered an unidentified X-Ray emission at around 3.5 keV in the stacked spectrum of 73 galaxy clusters, and one hypothesis to explain this new line is dark matter decay, especially the decay of sterile neutrinos in keV mass range. Although blank sky observations from XMM-Newton have declined this hypothesis [18], our work is motivated by a similar idea of monoenergetic dark matter decay into a single photon line.

In this work, we use a high-fidelity map of the loca-

tion of galaxies/dark matter to cross-correlate with the spectral map of the dark sky or faint background object observations to look for the additional spectral line that corresponds with monoenergetic dark matter decay in the optical range, based on a large dataset from Dark Energy Spectroscopic Instrumentation (DESI) [19–23]. As dark matter halos are extended much further compared with optically observable regions of galaxies, we target the far outskirts of the bright galaxies at redshift around 0.2 and of luminous red galaxies at redshift around 0.7 to avoid the influence of optical light. Compared with annihilation which follows the square of density profile ρ^2 , dark matter decay scales by ρ [24], which makes far outskirts of galaxies still a reasonable place to search for evidence. We stack the spectra at the rest-frame wavelength of corresponding galaxies to avoid observational or instrumental systematics that could arise at fixed observed wavelength. Although individual sources of dark matter are not detectable, we search for emission by determining its spatial cross-correlation function with accumulations of long exposure times.

This paper is structured as follows. In Section II we describe the data samples being used together with selection criteria and preparations. In Section III we present our methods for cross-correlation to obtain the stacked spectrum. We show our results in Section IV about line detection and the detection limit, and we compute the mass-luminosity relation for dark matter decay in Section V. Finally, we summarize and discuss the results further in Section VI.

II. DATA

This study makes use of data from the DESI survey, including the foreground galaxy position and redshift data and the spectra from both sky fibers and faint background galaxies. We use the data from the Year 1 data set, collected through June 2022, with processing via the “iron” version of the data compilation [25]. It will be released as part of DESI Data Release 1 (DR1), in a manner similar to that of the Early Data Release [26, 27].

We use the bright galaxies at low redshift from the Bright Galaxy Survey (BGS) [28]. The bright galaxies (BG) were selected based on three optical fluxes in the Legacy Surveys [29, 30], and we only select those that the redshift pipeline assesses to have bitmask $ZWARN = 0$, as these have been found to yield a robust set with few redshift errors. We choose 5914291 BGs in total with an average redshift of 0.24.

To enlarge the wavelength range of our search, massive galaxies at higher redshift are also selected from DESI Luminous Red Galaxy (LRG) Sample in the redshift range $0.3 < z \lesssim 1.0$ [31]. Target selection is based on Legacy Imaging Surveys Data Release 9 g, r, z and *WISE W1* photometry [29]. We make use of 2492017 LRGs in total with an average redshift of 0.72.

We then collect the sample of spectra from the dark-

time survey tiles that we will consider for stacking. The dark-time survey has longer exposures and lower moon contamination, so it is better for searching for faint signals. We seek spectra that have relatively little light from their intended target. Many such spectra exist because of the sky fibers, intentionally placed on areas that were blank in the optical imaging used for target selection [32]. But many DESI targets are also rather faint, and we opt to use these as well, provided that they are at a well-separated redshift. To keep the spectra in a faint enough level, the faint background galaxies are selected within a fiber total flux range of $F_G \leq 0.63$, $F_R \leq 1.0$, and $F_Z \leq 1.58$ in unit of nanomaggies. We do not use quasar targets, as these are often brighter and have more variations in their spectra. To avoid including spectral pixels from these spectra, we further pre-process the faint target spectra by masking wavelengths corresponding to strong oxygen and hydrogen emission lines at the redshift of the target. This is simply to avoid including pixels with large narrow-band lines that we know have a familiar physical cause, but that will add noise to the stack.

We convert the angular positions of the primary galaxy samples into Cartesian coordinates on a unit sphere and utilize the SciPy CKDTree method [33] to look for nearby sky or faint background objects as targets for the spectral map. We set a separation threshold of $20''$ to look for pairing within this angular distance range. When pairing with the faint background targets, we reject the pairs with similar redshift, $\|z_{\text{tgt}} - z_{\text{bgs}}\| < 0.05 \times (1 + z_{\text{bgs}})$, to sharply reduce any correlations with the primary object.

With this search, we find 80472 sky fiber spectra around the bright galaxies and 40659 sky fiber spectra around LRGs. We also find 437502 background galaxies fibers on faint background objects around BGs and 150958 background galaxies fibers around LRGs. For each pair, the spectra of the sky (or qualified faint galaxy targets) are shifted to the rest-frame wavelength of the corresponding primary galaxy. Fiber collision will suppress the number of pairs with small angular separation, but because DESI returns to one sky region multiple times with different targets, there are plenty of small-angle measurements and when averaging within the angular bin, the fiber collision effect will drop out.

III. CROSS-CORRELATION

To find the cross-correlation between the foreground galaxies and nearby spectra, we co-add all rest-frame spectra into a wavelength grid from 2000 Å to 10000 Å with 1 Å bins. Coaddition is done by assigning individual pixels from each spectrum into single bins of the final wavelength grid. The final stacked spectrum ξ after co-addition is given by

$$\xi = \frac{1}{\sum_{i=1}^N \omega_i} \sum_{i=1}^N \omega_i F_i, \quad (1)$$

where N is the total number of pixels in each bin of the grid, $\omega_i = 1/\sigma_i^2$ is the inverse variance of flux at each pixel, and F_i is the flux. Masked pixels are given the inverse variance of zero.

The coaddition is done with different classifications of the sample. Despite a general coaddition of all available pairs, we have also grouped the sample based on angular separation or physical separation between the pairs. The angular separation bins are logarithm ones from 2.5 to 20 arcsecond. The physical separation is calculated using a flat cosmological model with matter density $\Omega_m = 0.3$ and cosmological constant density $\Omega_\Lambda = 0.7$ at the redshift of the foreground galaxy in the pair, and then we use logarithm bins from 10 to 160 kpc.

We search for prominent lines in these stacked spectra. For each stack, we utilize a Savitzky–Golay filter with a window size of 205 Å to smooth the data and then remove the smoothing curve to rescale the average flux level around zero. Then, we convolve the spectrum with a 1D Gaussian kernel to calculate the line flux. We use two such kernels with different sizes. The primary narrow kernel with a standard deviation of 3 Å is physically motivated by the general line broadening of an intrinsically narrow line due to the normal velocity dispersion of halos of dark matter particles. However, the line could also be intrinsically broader. To investigate this possibility, we also make use of a broad kernel with a standard deviation of 15 Å. This kernel size is limited by the fact that the high-pass filtering needed to remove the continuum flux left over from the faint galaxies would artificially remove signals of broader lines.

The final step is to find the signal-to-noise ratio (SNR) at each wavelength. We first calculate the robust estimated error using half the interval between the 16% and 84% quantiles in subsets of data within 400 Å bins separated by 200 Å, and then fit a smooth curve with these points. The SNR is generated by the convolution spectrum over the error level. An example of this process is displayed in Figure 1, which shows the stacked spectrum for all sky fiber-bright galaxy pairs.

We constrain the wavelength range from 3000 Å to 9000 Å for BGs as most of the pairs could inform these wavelengths. For pairs with LRGs, we switch the wavelength range to 2000–7000 Å to take advantage of the higher redshift.

IV. RESULTS

We first focus on the bright galaxies at lower redshift. We show the SNR of all bright galaxy-sky fiber pairs and bright galaxy-faint background target pairs in Figure 2. We did not find unknown signals that might be correlated with dark matter decay in the galaxy halo, but we do recognize several famous spectral lines in the SNR of the cross-correlation between faint targets and bright galaxies, including the [OII] emission doublet at 3726 and 3729 Å, Calcium H and K absorption at 3969 and 3934 Å,

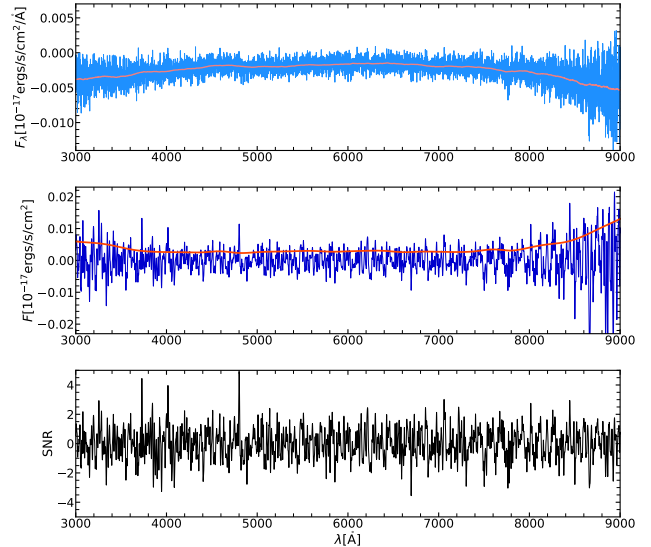


FIG. 1. An example of data processing for pairs of bright galaxies and sky fibers. The upper panel shows the original stacked spectrum after coaddition in blue, and the pink curve is the smoothed curve generated by the Savitzky–Golay filter. The middle panel (blue) shows the Gaussian convolution with a 3 Å kernel of the spectrum after subtracting the smooth continuum to find out the line flux. The red line is the estimated error curve from calculating half the interval between the 16% and 84% quantiles in successive subsets of adjacent data points. The last panel shows the signal to noise ratio.

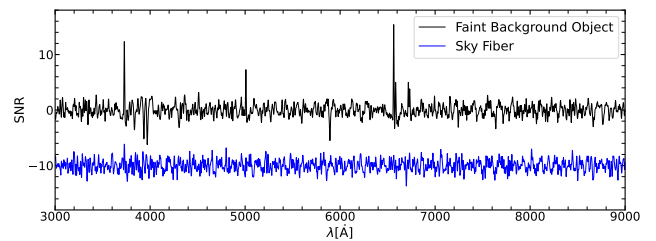


FIG. 2. The SNR of all pairs of bright galaxies and faint background objects in black and SNR of all sky pairs in blue. The SNR of sky pairs is shifted by -10 from 0 to -10 on the plot.

[OIII] lines at 4959 and 5007 Å, Sodium D absorption at 5890 and 5896 Å, H α at 6563 Å, [NII] at 6583 Å, and two lines from singly-ionized sulfur ([SII]) at 6716 and 6731 Å. Figure 3 shows a zoomed-in plot of the SNR around each prominent spectral line in angular separation and physical separation bins. The figures demonstrate that the line intensity is negatively correlated with the distance between the pair for the emissions. We propose the absorption features as coming from the circumgalactic gas. The emission lines are only seen when using background galaxies, rather than sky fibers, so we expect that these lines must come from emission that is superposed on the

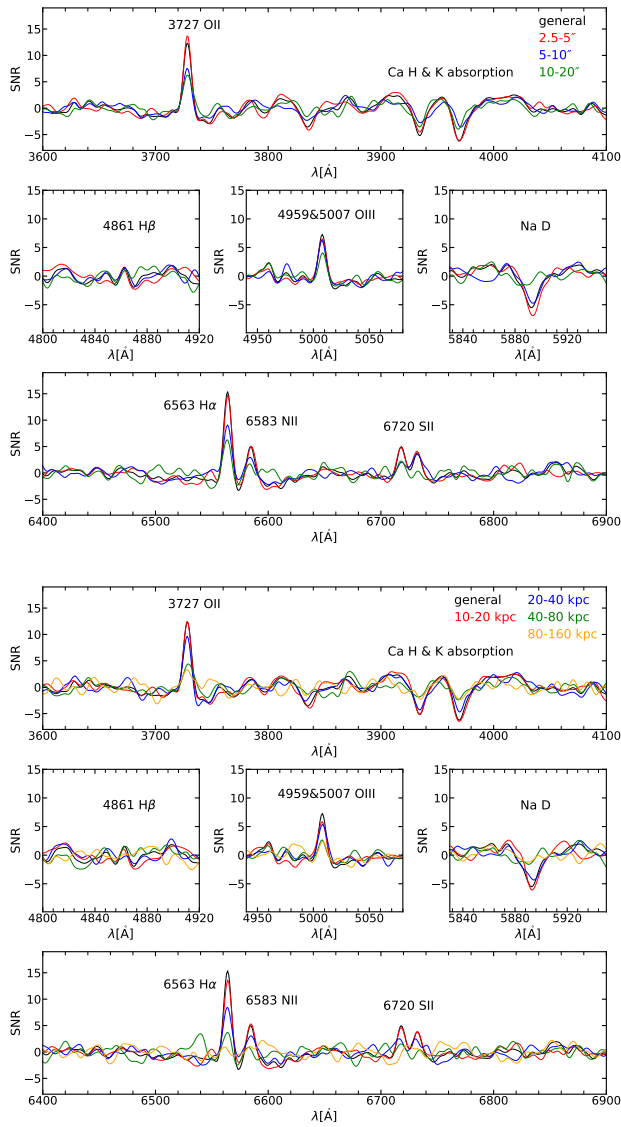


FIG. 3. The SNR of all available bright galaxy-faint background object pairs zoomed in around prominent lines. The upper panel shows the result in angular separation bins, and the lower panel shows the result in physical separation bins. The bins are specified on the upper-right corner of each panel. The black "General" curve is the sum of all available pairs with a separation below the threshold of $20''$.

background galaxy, but that would be rejected by the sky-fiber selection. Possible emission sources could be dwarf galaxies satellites, scattered light from the galactic center by the dust around the galaxy, or direct light from the extended gaseous halo. However, we are not able to infer surface brightness as a function of distance at the outskirts of the bright galaxies because these dark background target positions are not selected randomly around a sample from BGS. Rather, DESI is preferentially choosing fainter locations, such that we would de-select brighter satellites of the bright galaxy.

We repeat the same process for pairs with LRGs, and the comparison between stacked spectra is shown in Figure 4. In the enlarged wavelength range, the 2800 \AA magnesium absorption line from the circumgalactic medium is also visible. We see stronger magnesium absorption features compared with the spectrum of bright galaxy pairs, which makes sense as LRGs tend to reside in denser regions with more absorbing gases around. The emission features are less prominent because the dust scattered light from dwarf galaxy neighbors is the major source for emissions, but the interstellar mediums are hot around these massive galaxies and they do not have star-forming neighbors with strong emission features. Again, we are not able to interpret the difference in line intensities between the two groups directly due to the biased target selection algorithm.

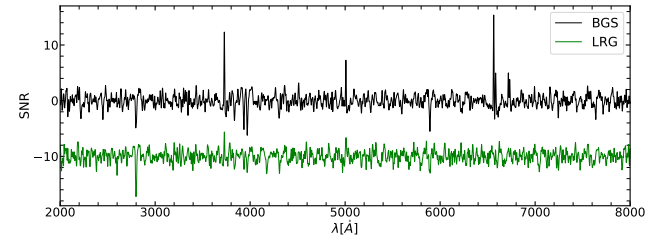


FIG. 4. Comparison between stacked spectrum of BG and LRG pairs at all separations. The SNR of LRG pairs are shifted by -10 from 0 to -10 on the plot.

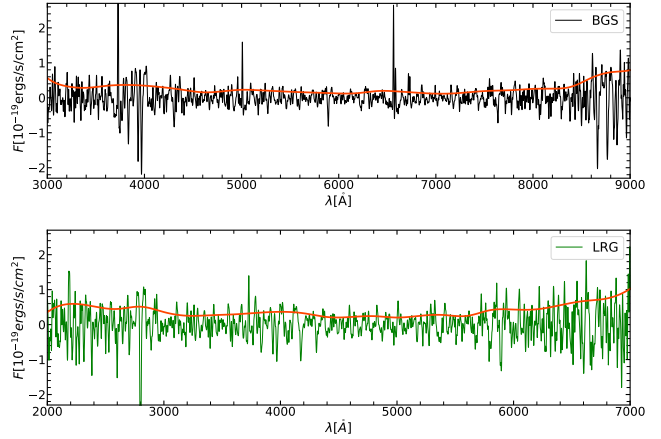


FIG. 5. The convolution spectra of all blank sky and faint background objects with foreground galaxies after coaddition. The upper panels show the BG pairs and the lower panel shows the LRG pairs. The red line shows the level of noise estimated by 68% error.

Instead, we are more interested in the general noise level of the flux density, which can be an indicator of our detection limit. We show in Figure 5 the overall level of error in the stacked spectrum from all BG and LRG pairs including those of sky objects and of dark background

targets. The result indicates that the uncertainty of flux is within $\pm 10^{-19}$ ergs/s/cm² for both groups.

Thus, the corresponding flux density in normal broadband centered at 5000 Å is

$$F_\nu = \frac{10^{-19} \text{ ergs/s/cm}^2}{1.5 \times 10^{14} \text{ Hz}} \quad (2)$$

$$\sim 10^{-33} \text{ ergs/s/cm}^2/\text{Hz} = 10^{-10} \text{ Jy}, \quad (3)$$

which is 33.9 in AB magnitude. The threshold magnitude for DESI BGS is 20 [34], and the faintest object observed in Hubble eXtreme Deep Field is at AB magnitude 31 [35]. Compared with these, our detection is much fainter than observable light from direct imaging.

With an angular diameter of 1.5'' of the DESI fiber, the line surface brightness (flux per unit solid angle) is around the level of 10^{-19} ergs/s/cm²/arcsec². Moreover, fluxes should be divided by 1.3 to undo the aperture corrections that were applied for point-source spectrophotometry. The 5σ detection limit for BG pairs is displayed in the upper panel of Figure 6. The level of 5σ detection limit of narrow line emissions estimated from the co-added spectra is 10^{-19} ergs/s/cm²/arcsec². For a singular isothermal sphere (SIS) density profile of $1/r^2$, we would expect the dark matter decay intensity in projection to drop as $1/r$. Therefore, we collapse across radius by weighting the spectra by $10''/r$, where r is the angular separation between the pair.

While the search is mainly designed for narrow-line emissions and chooses the primary kernel size according to the dispersal velocity of galaxies, we also estimate the detection limit for broader-line emissions by increasing the sizes for both the Savitzky–Golay filter and the Gaussian convolution kernel. In the bottom panel of Figure 6, we show the detection limit when using a Savitzky–Golay filter with window size 505 to remove the flux continuum and then a Gaussian convolution kernel with a width of 15 Å for the same sample of BG pairs.

We repeat the same process for LRG pairs. The weighted 5σ detection limit for narrow line emissions and broad line emissions and their comparison with those from the BGS group is shown in Figure 7. We set the wavelength range to 3000 – 7000 Å to focus at regions where the error is well-constrained for both galaxy groups. The detection limits for either narrow or broad lines are always similar for both pairings with BGs and LRGs, but the broad line detection behaves more poorly and shows more variability. This makes sense as the increase in the uncertainty of flux and the detection limit scale with the square root of the size of the convolution filter.

V. COMPUTATION OF DARK MATTER EMISSIVITY

The motivation of our search is to look for unidentified lines corresponding with dark matter decay. Compared with annihilation, the rate of which goes as the square of

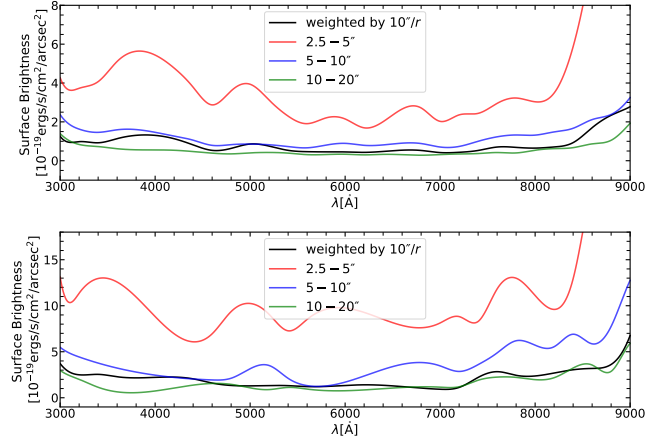


FIG. 6. The 5σ detection limit of surface brightness for narrow-line emission (top) and for broad-line emission (bottom) generally and in angular separation bins for all BG pairs. The general line is calculated from the sum of all spectra weighted by $10''/r$, which is the expected model for signal strength from dark matter decay. If re-scaling the detection limits in different angular bins with this model, they appear on similar levels, while the error in the 2.5–5'' separation bin is a little overestimated as there are a more limited number of pairs in this subset.

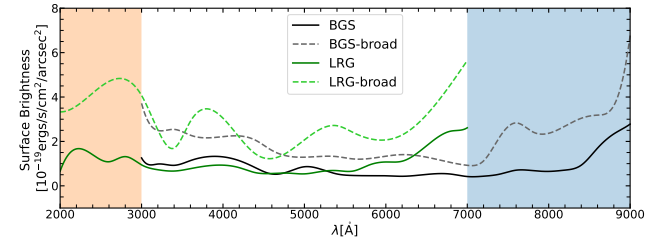


FIG. 7. Comparison between the 5σ detection limit of surface brightness for narrow or broad line searches for both BG and LRG pairs. The shaded regions show the cutoff in the selected wavelength for each group.

density, dark matter decay scales with the density profile, making the far outskirts of galaxies a viable place to search for signals. To interpret our detection limits in terms of a luminosity-to-mass ratio for dark matter particles, we will need to know the total mass of dark matter contributing to the measured surface brightness.

To estimate surface mass density associated with our line search, we need the results from galaxy-galaxy weak gravitational lensing [36]. As there are no measurements yet available with DESI BG or LRG samples, we use prior lensing signals detected with a similar flux-limited sample of low-redshift galaxy targets from the Sloan Digital Sky Survey (SDSS). Because our detection limits of surface brightness are similar for BGs and LRGs, focusing the calculation on the group with more reliable surface mass density measurement is sufficient here. From the Galaxy-Mass Correlation Function measured from weak

lensing of galaxies in the main sample of SDSS, the surface mass density $\Sigma(R) \sim 20 M_\odot/\text{pc}^2 \sim 0.004 \text{ g/cm}^2$ at $R = 150 \text{ kpc}$ [37].

If the dark matter had a line luminosity per unit mass of ϵ_{DM} , then this mass overdensity around the galaxies would produce a line flux in our apertures of solid angle Ω of

$$F = \frac{\Omega \epsilon_{\text{DM}} \Sigma(R)}{4\pi(1+z)^4} \quad (4)$$

where the $(1+z)^4$ arises from cosmological surface brightness dimming. Inserting the measured surface density and using $z \approx 0.2$, we find that our line flux limits correspond to a limit on $\epsilon_{\text{DM}} \sim 3 \times 10^{-5} \text{ ergs/s/g}$.

This is a very small emissivity, likely undetectable in terrestrial experiments. For instance, given the dark matter density of $\sim 10^{-25} \text{ g/cm}^3$ in our solar system [38], the emissivity of dark matter decay is at a level of 10^{-12} photons per second per cubic meter.

When integrating along the line of sight to find the total mass of dark matter contributing to luminosity, it is possible to compare our detection limit with the extragalactic background light (EBL). For a specific wavelength,

$$\text{SB}_\lambda \sim \epsilon_{\text{DM}} \frac{c}{H(z)} \frac{D_A^2(1+z)^2}{4\pi D_L^2} \rho_{\text{DM}} \frac{\delta z}{\lambda_0} \quad (5)$$

$$\sim 10^{-15} \text{ ergs/s/cm}^2/\text{arcsec}^2/\text{\AA}, \quad (6)$$

using the average dark matter density of the universe $\rho_{\text{DM}} = 2.1 \times 10^{-30} \text{ g/cm}^3$, and the general surface brightness after integration is

$$\text{SB} = \int_{z_1}^{z_2} \epsilon_{\text{DM}} \frac{c}{H(z)} \frac{D_A^2(1+z)^2}{4\pi D_L^2} \rho_{\text{DM}} dz \quad (7)$$

$$\sim \frac{c}{4\pi H_0} \epsilon_{\text{DM}} \rho_{\text{DM}} \sim 10^{-18} \text{ ergs/s/cm}^2/\text{arcsec}^2. \quad (8)$$

The EBL measured by total optical light subtracting zodiacal light (ZL) and diffuse Galactic light (DGL) is on the order of magnitude of $10^{-9} \text{ ergs/s/cm}^2/\text{sr}/\text{\AA}$ in a 4000–7000 Å filter [39], which corresponds to a surface brightness around $10^{-16} \text{ ergs/s/cm}^2/\text{arcsec}^2$. This shows that our detection is two orders of magnitude fainter than the EBL.

If we repeat the calculation inside the Milky Way with a SIS density profile normalized at the density at the solar circle, the surface brightness after integration along a line sight perpendicular to the galactic plane is

$$\text{SB} = \int \epsilon_{\text{DM}} \frac{\rho_{\text{DM,solar}} \cdot (8 \text{ kpc}/r)^2}{4\pi z^2} z^2 dz \quad (9)$$

$$\sim 2 \times 10^{-19} \text{ ergs/s/cm}^2/\text{arcsec}^2, \quad (10)$$

where z is the axis perpendicular to the galactic plane, and $r^2 = z^2 + (8 \text{ kpc})^2$.

If spreading the flux over the 3 Å Gaussian convolution kernel, the peak line surface brightness in the filter is estimated as

$$\text{SB}_\lambda \sim 3 \times 10^{-20} \text{ ergs/s/cm}^2/\text{arcsec}^2/\text{\AA}. \quad (11)$$

The optical dark-sky background is normally at AB magnitude of 22 per square arcsecond, which corresponds to a flux density of about $10^{-5} \text{ Jy/arcsec}^2$. Then,

$$F_{\lambda,\text{sky}} = \frac{\nu}{\lambda} F_{\nu,\text{sky}} \sim 10^{-17} \text{ ergs/s/cm}^2/\text{arcsec}^2/\text{\AA}. \quad (12)$$

Hence, the potential signal level is over two orders of magnitude lower than the sky background. With such low signal strength, given a blank sky spectrum, it can be hard to distinguish whether the anomalous contribution is from atmosphere, back scattered light from the sun, scattered light from the galaxy and interstellar medium, or actually dark matter decay in the halo. Most practical observations subtract the sky differentially in angle, making the signal hard to detect.

VI. DISCUSSION

In this work, we use positions of galaxies/dark matter to cross-correlate the spectral map of sky and faint background object emissions with DESI Y1 data. The spatial cross-correlation function gives no evidence of unidentified spectral lines caused by dark matter decay, but we obtain a detection limit for any potential narrow line emission from dark matter on the order of magnitude of $10^{-19} \text{ ergs/s/cm}^2/\text{arcsec}^2$. This corresponds with 34 in normal broadband in the AB magnitude system. The mass-luminosity relation estimated from the surface mass density of galaxies indicates that dark matter decay can produce at most 10^{-5} photon per year in a cubic meter on Earth. It is also suggested that the total surface brightness contributed by all dark matter integrated along the line of sight is orders of magnitude fainter than the observed extragalactic background light.

NASA's New Horizons spacecraft has measured an anomalous component of flux coming from unknown origins at the level of $10^{-16} \text{ ergs/s/cm}^2/\text{arcsec}^2$ in the cosmic optical background (COB) using images of New Horizons' Long Range Reconnaissance Imager (LORRI) [40, 41]. One hypothetical source of this extra flux is dark matter decay and Line Intensity Mapping (LIM) is suggested as a useful tool for detection [42–44]. However, the integrated surface brightness calculated with our detection limit from the co-added spectra of over three hundred thousand pairs is also two orders of magnitude lower than the observed level of the anomalous flux, which makes this hypothesis unlikely. Therefore, we suggest that narrow-line emissions from dark matter decay cannot be the major source of the EBL.

One caveat of the conclusion is that we are only looking at the wavelength range from 3000 to 9000 Å, as we perform calculations with bright galaxies at relatively low

redshift. However, the extra light in the COB could also be coming from for example an ultraviolet line at higher redshift. It is possible to enlarge the wavelength range of the search by cross-correlating with objects at higher redshift, such as emission line galaxies (ELGs). We have tried to cross-correlate with LRGs but the flux error level is quite similar, and it does not provide any further insight into the detection limit. We would also need to measure the proper weak lensing signals from the DESI BGS sample to get a more accurate mass-luminosity relation and from there try to target at regions with more dark matter, such as in pairs or triples of the large galaxies, which can provide significant improvement in the signal strength.

ACKNOWLEDGEMENT

We thank Tracy Slatyer and Doug Finkbeiner for useful conversations. H.W. was supported by the Harvard College Research Program. D.J.E. was supported by U.S. Department of Energy grant DE-SC0007881 and as a Simons Foundation Investigator. This research used resources of the National Energy Research Scientific Computing Center (NERSC), a U.S. Department of Energy Office of Science User Facility located at Lawrence Berkeley National Laboratory, operated under Contract No. DE-AC02-05CH11231.

This material is based upon work supported by the U.S. Department of Energy (DOE), Office of Science,

Office of High-Energy Physics, under Contract No. DE-AC02-05CH11231, and by the National Energy Research Scientific Computing Center, a DOE Office of Science User Facility under the same contract. Additional support for DESI was provided by the U.S. National Science Foundation (NSF), Division of Astronomical Sciences under Contract No. AST-0950945 to the NSF's National Optical-Infrared Astronomy Research Laboratory; the Science and Technology Facilities Council of the United Kingdom; the Gordon and Betty Moore Foundation; the Heising-Simons Foundation; the French Alternative Energies and Atomic Energy Commission (CEA); the National Council of Science and Technology of Mexico (CONACYT); the Ministry of Science and Innovation of Spain (MICINN), and by the DESI Member Institutions: <https://www.desi.lbl.gov/collaborating-institutions>. Any opinions, findings, and conclusions or recommendations expressed in this material are those of the author(s) and do not necessarily reflect the views of the U. S. National Science Foundation, the U. S. Department of Energy, or any of the listed funding agencies.

The authors are honored to be permitted to conduct scientific research on Iolkam Du'ag (Kitt Peak), a mountain with particular significance to the Tohono O'odham Nation.

DATA AVAILABILITY

All data points shown in the published graphs are available in machine-readable form in Zenodo at <https://doi.org/10.5281/zenodo.8339781>.

-
- [1] S. Dodelson and L. M. Widrow, Sterile neutrinos as dark matter, *Phys. Rev. Lett.* **72**, 17 (1994), arXiv:hep-ph/9303287 [hep-ph].
 - [2] T. Moroi, Effects of the Gravitino on the Inflationary Universe, arXiv e-prints , hep-ph/9503210 (1995), arXiv:hep-ph/9503210 [hep-ph].
 - [3] L. Covi, J. E. Kim, and L. Roszkowski, Axinos as Cold Dark Matter, *Phys. Rev. Lett.* **82**, 4180 (1999), arXiv:hep-ph/9905212 [hep-ph].
 - [4] J. Preskill, M. B. Wise, and F. Wilczek, Cosmology of the invisible axion, *Physics Letters B* **120**, 127 (1983).
 - [5] L. Abbott and P. Sikivie, A cosmological bound on the invisible axion, *Physics Letters B* **120**, 133 (1983).
 - [6] C. El Aisati, M. Gustafsson, T. Hambye, and T. Scarna, Dark matter decay to a photon and a neutrino: The double monochromatic smoking gun scenario, *Phys. Rev. D* **93**, 043535 (2016), arXiv:1510.05008 [hep-ph].
 - [7] G. Carosi, A. Friedland, M. Giannotti, M. J. Pivovaroff, J. Ruz, and J. K. Vogel, Probing the axion-photon coupling: phenomenological and experimental perspectives. A snowmass white paper, arXiv e-prints , arXiv:1309.7035 (2013), arXiv:1309.7035 [hep-ph].
 - [8] M. H. Chan, Constraining the axion-photon coupling using radio data of the Bullet cluster, *Scientific Reports* **11**, 20087 (2021), arXiv:2109.11734 [astro-ph.CO].
 - [9] C. Balázs, S. Bloor, T. E. Gonzalo, W. Handley, S. Hoof, F. Kahlhoefer, M. Lecroq, D. J. E. Marsh, J. J. Renk, P. Scott, and P. Stöcker, Cosmological constraints on decaying axion-like particles: a global analysis, arXiv e-prints , arXiv:2205.13549 (2022), arXiv:2205.13549 [astro-ph.CO].
 - [10] A. Kusenko, Sterile neutrinos: The dark side of the light fermions, *Physics Reports* **481**, 1 (2009).
 - [11] D. O. Caldwell, R. M. Eisberg, D. M. Grumm, M. S. Witherell, B. Sadoulet, F. S. Goulding, and A. R. Smith, Laboratory limits on galactic cold dark matter, *Phys. Rev. Lett.* **61**, 510 (1988).
 - [12] T. Marrodán Undagoitia, W. Rodejohann, T. Wolf, and C. E. Yaguna, Laboratory limits on the annihilation or decay of dark matter particles, *Progress of Theoretical and Experimental Physics* **2022**, 013F01 (2022), arXiv:2107.05685 [hep-ph].
 - [13] J. Hubert, A. Schneider, D. Potter, J. Stadel, and S. K. Giri, Decaying dark matter: simulations and weak-lensing forecast, *J. Cosmology Astropart. Phys.* **2021**, 040 (2021), arXiv:2104.07675 [astro-ph.CO].
 - [14] O. Ruchayskiy, A. Boyarsky, D. Iakubovskyi, E. Bulbul, D. Eckert, J. Franse, D. Malyshev, M. Markevitch, and A. Neronov, Searching for decaying dark matter in deep XMM-Newton observation of the Draco dwarf

- spheroidal, MNRAS **460**, 1390 (2016), arXiv:1512.07217 [astro-ph.HE].
- [15] S. Ando and K. Ishiwata, Constraints on decaying dark matter from the extragalactic gamma-ray background, J. Cosmology Astropart. Phys. **2015**, 024 (2015), arXiv:1502.02007 [astro-ph.CO].
- [16] K. Abazajian, Detection of Dark Matter Decay in the X-ray, in *astro2010: The Astronomy and Astrophysics Decadal Survey*, Vol. 2010 (2009) p. 1, arXiv:0903.2040 [astro-ph.CO].
- [17] E. Bulbul, M. Markevitch, A. Foster, R. K. Smith, M. Loewenstein, and S. W. Randall, Detection of an Unidentified Emission Line in the Stacked X-Ray Spectrum of Galaxy Clusters, ApJ **789**, 13 (2014), arXiv:1402.2301 [astro-ph.CO].
- [18] C. Dessert, N. L. Rodd, and B. R. Safdi, The dark matter interpretation of the 3.5-keV line is inconsistent with blank-sky observations, Science **367**, 1465 (2020), arXiv:1812.06976 [astro-ph.CO].
- [19] DESI Collaboration, A. Aghamousa, J. Aguilar, S. Ahlen, S. Alam, L. E. Allen, C. Allende Prieto, J. Annis, S. Bailey, C. Balland, O. Ballester, C. Battay, L. Beaufore, C. Bebek, T. C. Beers, E. F. Bell, J. L. Bernal, R. Besuner, F. Beutler, C. Blake, H. Bleuler, M. Blomqvist, R. Blum, A. S. Bolton, C. Briceno, D. Brooks, J. R. Brownstein, E. Buckley-Geer, A. Burden, E. Burtin, N. G. Busca, R. N. Cahn, Y.-C. Cai, L. Cardiel-Sas, R. G. Carlberg, P.-H. Carton, R. Casas, F. J. Castander, J. L. Cervantes-Cota, T. M. Claybaugh, M. Close, C. T. Coker, S. Cole, J. Comparat, A. P. Cooper, M. C. Cousinou, M. Crocce, J.-G. Cuby, D. P. Cunningham, T. M. Davis, K. S. Dawson, A. de la Macorra, J. De Vicente, T. Delubac, M. Derwent, A. Dey, G. Dhungana, Z. Ding, P. Doel, Y. T. Duan, A. Ealet, J. Edelstein, S. Eftekharzadeh, D. J. Eisenstein, A. El-lliott, S. Escoffier, M. Evatt, P. Fagrelius, X. Fan, K. Fanning, A. Farahi, J. Farihi, G. Favole, Y. Feng, E. Fernandez, J. R. Findlay, D. P. Finkbeiner, M. J. Fitzpatrick, B. Flaugher, S. Flender, A. Font-Ribera, J. E. Forero-Romero, P. Fosalba, C. S. Frenk, M. Fumagalli, B. T. Gaensicke, G. Gallo, J. Garcia-Bellido, E. Gaztanaga, N. Pietro Gentile Fusillo, T. Gerard, I. Gershkovich, T. Giannantonio, D. Gillet, G. Gonzalez-de-Rivera, V. Gonzalez-Perez, S. Gott, O. Graur, G. Gutierrez, J. Guy, S. Habib, H. Heetderks, I. Heetderks, K. Heitmann, W. A. Hellwing, D. A. Herrera, S. Ho, S. Holland, K. Honscheid, E. Huff, T. A. Hutchinson, D. Huterer, H. S. Hwang, J. M. Illa Laguna, Y. Ishikawa, D. Jacobs, N. Jeffrey, P. Jelinsky, E. Jennings, L. Jiang, J. Jimenez, J. Johnson, R. Joyce, E. Jullo, S. Juneau, S. Kama, A. Karcher, S. Karkar, R. Kehoe, N. Kennamer, S. Kent, M. Kilbinger, A. G. Kim, D. Kirkby, T. Kisner, E. Kitaniidis, J.-P. Kneib, S. Koposov, E. Kovacs, K. Koyama, A. Kremin, R. Kron, L. Kronig, A. Kueter-Young, C. G. Lacey, R. Lafever, O. Lahav, A. Lambert, M. Lampton, M. Landriau, D. Lang, T. R. Lauer, J.-M. Le Goff, L. Le Guillou, A. Le Van Suu, J. H. Lee, S.-J. Lee, D. Leitner, M. Lesser, M. E. Levi, B. L'Huillier, B. Li, M. Liang, H. Lin, E. Linder, S. R. Loebman, Z. Lukic, J. Ma, N. MacCrann, C. Magneville, L. Makarem, M. Manera, C. J. Manser, R. Marshall, P. Martini, R. Massey, T. Matheson, J. McCauley, P. McDonald, I. D. McGreer, A. Meisner, N. Metcalfe, T. N. Miller, R. Miquel, J. Moustakas, A. Myers, M. Naik, J. A. Newman, R. C. Nichol, A. Nicola, L. Nicolati da Costa, J. Nie, G. Niz, P. Norberg, B. Nord, D. Norman, P. Nugent, T. O'Brien, M. Oh, K. A. G. Olsen, C. Padilla, H. Padmanabhan, N. Padmanabhan, N. Palanque-Delabrouille, A. Palmese, D. Pappalardo, I. Paris, C. Park, A. Patej, J. A. Peacock, H. V. Peiris, X. Peng, W. J. Percival, S. Perruchot, M. M. Pieri, R. Pogge, J. E. Pollock, C. Poppett, F. Prada, A. Prakash, R. G. Probst, D. Rabinowitz, A. Raichoor, C. H. Ree, A. Refregier, X. Regal, B. Reid, K. Reil, M. Rezaie, C. M. Rockosi, N. Roe, S. Ronayette, A. Roodman, A. J. Ross, N. P. Ross, G. Rossi, E. Rozo, V. Ruhlmann-Kleider, E. S. Rykoff, C. Sabiu, L. Samushia, E. Sanchez, J. Sanchez, D. J. Schlegel, M. Schneider, M. Schubnell, A. Secroun, U. Seljak, H.-J. Seo, S. Serrano, A. Shafieloo, H. Shan, R. Sharples, M. J. Sholl, W. V. Shourt, J. H. Silber, D. R. Silva, M. M. Sirk, A. Slosar, A. Smith, G. F. Smoot, D. Som, Y.-S. Song, D. Sprayberry, R. Staten, A. Stefanik, G. Tarle, S. Sien Tie, J. L. Tinker, R. Tojeiro, F. Valdes, O. Valenzuela, M. Valluri, M. Vargas-Magana, L. Verde, A. R. Walker, J. Wang, Y. Wang, B. A. Weaver, C. Weaverdyck, R. H. Wechsler, D. H. Weinberg, M. White, Q. Yang, C. Yeeche, T. Zhang, G.-B. Zhao, Y. Zheng, X. Zhou, Z. Zhou, Y. Zhu, H. Zou, and Y. Zu, The DESI Experiment Part I: Science, Targeting, and Survey Design, arXiv e-prints , arXiv:1611.00036 (2016), arXiv:1611.00036 [astro-ph.IM].
- [20] DESI Collaboration, A. Aghamousa, J. Aguilar, S. Ahlen, S. Alam, L. E. Allen, C. Allende Prieto, J. Annis, S. Bailey, C. Balland, O. Ballester, C. Battay, L. Beaufore, C. Bebek, T. C. Beers, E. F. Bell, J. L. Bernal, R. Besuner, F. Beutler, C. Blake, H. Bleuler, M. Blomqvist, R. Blum, A. S. Bolton, C. Briceno, D. Brooks, J. R. Brownstein, E. Buckley-Geer, A. Burden, E. Burtin, N. G. Busca, R. N. Cahn, Y.-C. Cai, L. Cardiel-Sas, R. G. Carlberg, P.-H. Carton, R. Casas, F. J. Castander, J. L. Cervantes-Cota, T. M. Claybaugh, M. Close, C. T. Coker, S. Cole, J. Comparat, A. P. Cooper, M. C. Cousinou, M. Crocce, J.-G. Cuby, D. P. Cunningham, T. M. Davis, K. S. Dawson, A. de la Macorra, J. De Vicente, T. Delubac, M. Derwent, A. Dey, G. Dhungana, Z. Ding, P. Doel, Y. T. Duan, A. Ealet, J. Edelstein, S. Eftekharzadeh, D. J. Eisenstein, A. El-lliott, S. Escoffier, M. Evatt, P. Fagrelius, X. Fan, K. Fanning, A. Farahi, J. Farihi, G. Favole, Y. Feng, E. Fernandez, J. R. Findlay, D. P. Finkbeiner, M. J. Fitzpatrick, B. Flaugher, S. Flender, A. Font-Ribera, J. E. Forero-Romero, P. Fosalba, C. S. Frenk, M. Fumagalli, B. T. Gaensicke, G. Gallo, J. Garcia-Bellido, E. Gaztanaga, N. Pietro Gentile Fusillo, T. Gerard, I. Gershkovich, T. Giannantonio, D. Gillet, G. Gonzalez-de-Rivera, V. Gonzalez-Perez, S. Gott, O. Graur, G. Gutierrez, J. Guy, S. Habib, H. Heetderks, I. Heetderks, K. Heitmann, W. A. Hellwing, D. A. Herrera, S. Ho, S. Holland, K. Honscheid, E. Huff, T. A. Hutchinson, D. Huterer, H. S. Hwang, J. M. Illa Laguna, Y. Ishikawa, D. Jacobs, N. Jeffrey, P. Jelinsky, E. Jennings, L. Jiang, J. Jimenez, J. Johnson, R. Joyce, E. Jullo, S. Juneau, S. Kama, A. Karcher, S. Karkar, R. Kehoe, N. Kennamer, S. Kent, M. Kilbinger, A. G. Kim, D. Kirkby, T. Kisner, E. Kitaniidis, J.-P. Kneib, S. Koposov, E. Kovacs, K. Koyama, A. Kremin, R. Kron, L. Kronig, A. Kueter-Young, C. G. Lacey, R. Lafever, O. Lahav, A. Lambert, M. Lampton, M. Landriau, D. Lang, T. R. Lauer, J.-M. Le Goff, L. Le Guillou, A. Le Van Suu, J. H. Lee, S.-J. Lee, D. Leitner, M. Lesser, M. E. Levi, B. L'Huillier, B. Li, M. Liang, H. Lin, E. Linder, S. R. Loebman, Z. Lukic, J. Ma, N. MacCrann, C. Magneville, L. Makarem, M. Manera, C. J. Manser, R. Marshall, P. Martini, R. Massey, T. Matheson, J. McCauley, P. McDonald, I. D. McGreer, A. Meisner, N. Metcalfe, T. N. Miller, R. Miquel, J. Moustakas, A. Myers, M. Naik, J. A. Newman,

- Guillou, A. Le Van Suu, J. H. Lee, S.-J. Lee, D. Leitner, M. Lesser, M. E. Levi, B. L'Huillier, B. Li, M. Liang, H. Lin, E. Linder, S. R. Loebman, Z. Lukic, J. Ma, N. MacCrann, C. Magneville, L. Makarem, M. Manera, C. J. Manser, R. Marshall, P. Martini, R. Massey, T. Matheson, J. McCauley, P. McDonald, I. D. McGreer, A. Meisner, N. Metcalfe, T. N. Miller, R. Miquel, J. Moustakas, A. Myers, M. Naik, J. A. Newman, R. C. Nichol, A. Nicola, L. Nicolati da Costa, J. Nie, G. Niz, P. Norberg, B. Nord, D. Norman, P. Nugent, T. O'Brien, M. Oh, K. A. G. Olsen, C. Padilla, H. Padmanabhan, N. Padmanabhan, N. Palanque-Delabrouille, A. Palmese, D. Pappalardo, I. Paris, C. Park, A. Patej, J. A. Peacock, H. V. Peiris, X. Peng, W. J. Percival, S. Perruchot, M. M. Pieri, R. Pogge, J. E. Pollack, C. Poppett, F. Prada, A. Prakash, R. G. Probst, D. Rabinowitz, A. Raichoor, C. H. Ree, A. Refregier, X. Regal, B. Reid, K. Reil, M. Rezaie, C. M. Rockosi, N. Roe, S. Ronayette, A. Roodman, A. J. Ross, N. P. Ross, G. Rossi, E. Rozo, V. Ruhlmann-Kleider, E. S. Rykoff, C. Sabiu, L. Samushia, E. Sanchez, J. Sanchez, D. J. Schlegel, M. Schneider, M. Schubnell, A. Secroun, U. Seljak, H.-J. Seo, S. Serrano, A. Shafieloo, H. Shan, R. Sharples, M. J. Sholl, W. V. Shourt, J. H. Silber, D. R. Silva, M. M. Sirk, A. Slosar, A. Smith, G. F. Smoot, D. Som, Y.-S. Song, D. Sprayberry, R. Staten, A. Stefanik, G. Tarle, S. Sien Tie, J. L. Tinker, R. Tojeiro, F. Valdes, O. Valenzuela, M. Valluri, M. Vargas-Magana, L. Verde, A. R. Walker, J. Wang, Y. Wang, B. A. Weaver, C. Weaverdyck, R. H. Wechsler, D. H. Weinberg, M. White, Q. Yang, C. Yèche, T. Zhang, G.-B. Zhao, Y. Zheng, X. Zhou, Z. Zhou, Y. Zhu, H. Zou, and Y. Zu, The DESI Experiment Part II: Instrument Design, arXiv e-prints , arXiv:1611.00037 (2016), arXiv:1611.00037 [astro-ph.IM].
- [21] DESI Collaboration, B. Abareshi, J. Aguilar, S. Ahlen, S. Alam, D. M. Alexander, R. Alfarsy, L. Allen, C. Allende Prieto, O. Alves, J. Ameel, E. Armengaud, J. Asorey, A. Aviles, S. Bailey, A. Balaguera-Antolínez, O. Ballester, C. Baltay, A. Bault, S. F. Beltran, B. Benavides, S. BenZvi, A. Berti, R. Besuner, F. Beutler, D. Bianchi, C. Blake, P. Blanc, R. Blum, A. Bolton, S. Bose, D. Bramall, S. Brienden, A. Brodzeller, D. Brooks, C. Brownell, E. Buckley-Geer, R. N. Cahn, Z. Cai, R. Canning, R. Capasso, A. Carnero Rosell, P. Carton, R. Casas, F. J. Castander, J. L. Cervantes-Cota, S. Chabanier, E. Chaussidon, C. Chuang, C. Circosta, S. Cole, A. P. Cooper, L. da Costa, M. C. Cousinou, A. Cuceu, T. M. Davis, K. Dawson, R. de la Cruz-Noriega, A. de la Macorra, A. de Mattia, J. Della Costa, P. Demmer, M. Derwent, A. Dey, B. Dey, G. Dhungana, Z. Ding, C. Dobson, P. Doel, J. Donald-McCann, J. Donaldson, K. Douglass, Y. Duan, P. Dunlop, J. Edelstein, S. Eftekharzadeh, D. J. Eisenstein, M. Enriquez-Vargas, S. Escoffier, M. Evatt, P. Fagrelius, X. Fan, K. Fanning, V. A. Fawcett, S. Ferraro, J. Ereza, B. Flaugher, A. Font-Ribera, J. E. Forero-Romero, C. S. Frenk, S. Fromenteau, B. T. Gänsicke, C. Garcia-Quintero, L. Garrison, E. Gaztañaga, F. Gerardi, H. Gil-Marín, S. Gontcho a Gontcho, A. X. Gonzalez-Morales, G. Gonzalez-de-Rivera, V. Gonzalez-Perez, C. Gordon, O. Graur, D. Green, C. Grove, D. Gruen, G. Gutierrez, J. Guy, C. Hahn, S. Harris, D. Herrera, H. K. Herrera-Alcantar, K. Honscheid, C. Howlett, D. Huterer, V. Iršić, M. Ishak, P. Jelinsky, L. Jiang, J. Jimenez, Y. P. Jing, R. Joyce, E. Jullo, S. Juneau, N. G. Karaçaylı, M. Karamanis, A. Karcher, T. Karim, R. Kehoe, S. Kent, D. Kirkby, T. Kisner, F. Kitaura, S. E. Koposov, A. Kovács, A. Kremin, A. Krolewski, B. L'Huillier, O. Lahav, A. Lambert, C. Lamman, T.-W. Lan, M. Landriau, S. Lane, D. Lang, J. U. Lange, J. Lasker, L. Le Guillou, A. Leauthaud, A. Le Van Suu, M. E. Levi, T. S. Li, C. Magneville, M. Manera, C. J. Manser, B. Marshall, P. Martini, W. McCollam, P. McDonald, A. M. Meisner, J. Mena-Fernández, J. Meneses-Rizo, M. Mezcua, T. Miller, R. Miquel, P. Montero-Camacho, J. Moon, J. Moustakas, E. Mueller, A. Muñoz-Gutiérrez, A. D. Myers, S. Nadathur, J. Najita, L. Napolitano, E. Neilsen, J. A. Newman, J. D. Nie, Y. Ning, G. Niz, P. Norberg, H. E. Noriega, T. O'Brien, A. Obuljen, N. Palanque-Delabrouille, A. Palmese, P. Zhiwei, D. Pappalardo, X. PENG, W. J. Percival, S. Perruchot, R. Pogge, C. Poppett, A. Porredon, F. Prada, J. Prochaska, R. Pucha, A. Pérez-Fernández, I. Pérez-Ràfols, D. Rabinowitz, A. Raichoor, S. Ramirez-Solano, C. Ramírez-Pérez, C. Ravoux, K. Reil, M. Rezaie, A. Rocher, C. Rockosi, N. A. Roe, A. Roodman, A. J. Ross, G. Rossi, R. Ruggeri, V. Ruhlmann-Kleider, C. G. Sabiu, S. Safanova, K. Said, A. Saintonge, J. Salas Catonga, L. Samushia, E. Sanchez, C. Saulder, E. Schaun, E. Schlafly, D. Schlegel, J. Schmoll, D. Scholte, M. Schubnell, A. Secroun, H. Seo, S. Serrano, R. M. Sharples, M. J. Sholl, J. H. Silber, D. R. Silva, M. Sirk, M. Siudek, A. Smith, D. Sprayberry, R. Staten, B. Stupak, T. Tan, G. Tarlé, S. S. Tie, R. Tojeiro, L. A. Ureña-López, F. Valdes, O. Valenzuela, M. Valluri, M. Vargas-Magaña, L. Verde, M. Walther, B. Wang, M. S. Wang, B. A. Weaver, C. Weaverdyck, R. Wechsler, M. J. Wilson, J. Yang, Y. Yu, S. Yuan, C. Yèche, H. Zhang, K. Zhang, C. Zhao, R. Zhou, Z. Zhou, H. Zou, J. Zou, S. Zou, Y. Zu, and DESI Collaboration, Overview of the Instrumentation for the Dark Energy Spectroscopic Instrument, AJ **164**, 207 (2022), arXiv:2205.10939 [astro-ph.IM].
- [22] J. H. Silber, P. Fagrelius, K. Fanning, M. Schubnell, J. N. Aguilar, S. Ahlen, J. Ameel, O. Ballester, C. Baltay, C. Bebek, D. Benton Beard, R. Besuner, L. Cardiel-Sas, R. Casas, F. J. Castander, T. Claybaugh, C. Dobson, Y. Duan, P. Dunlop, J. Edelstein, W. T. Emmet, A. Elliott, M. Evatt, I. Gershkovich, J. Guy, S. Harris, H. Heetderks, I. Heetderks, K. Honscheid, J. M. Illa, P. Jelinsky, S. R. Jelinsky, J. Jimenez, A. Karcher, S. Kent, D. Kirkby, J.-P. Kneib, A. Lambert, M. Lampert, D. Leitner, M. Levi, J. McCauley, A. Meisner, T. N. Miller, R. Miquel, J. Mundet, C. Poppett, D. Rabinowitz, K. Reil, D. Roman, D. Schlegel, S. Serrano, W. Van Shourt, D. Sprayberry, G. Tarlé, S. S. Tie, C. Weaverdyck, K. Zhang, M. Azzaro, S. Bailey, S. Becciril, T. Blackwell, M. Bouri, D. Brooks, E. Buckley-Geer, J. P. Castro, M. Derwent, A. Dey, G. Dhungana, P. Doel, D. J. Eisenstein, N. Fahim, J. Garcia-Bellido, E. Gaztañaga, S. G. A Gontcho, G. Gutierrez, P. Hörl, R. Kehoe, T. Kisner, A. Kremin, L. Kronig, M. Landriau, L. Le Guillou, P. Martini, J. Moustakas, N. Palanque-Delabrouille, X. Peng, W. Percival, F. Prada, C. Allende Prieto, G. G. de Rivera, E. Sanchez, J. Sanchez, R. Sharples, M. Soares-Santos, E. Schlafly, B. A. Weaver, Z. Zhou, Y. Zhu, H. Zou, and DESI Collaboration, The Robotic Multiobject Focal Plane System of the Dark En-

- ergy Spectroscopic Instrument (DESI), *AJ* **165**, 9 (2023), arXiv:2205.09014 [astro-ph.IM].
- [23] T. N. Miller, P. Doel, G. Gutierrez, R. Besuner, D. Brooks, G. Gallo, H. Heetderks, P. Jelinsky, S. M. Kent, M. Lampton, M. Levi, M. Liang, A. Meisner, M. J. Sholl, J. H. Silber, D. Sprayberry, J. N. Aguilar, A. de la Macorra, D. Eisenstein, K. Fanning, A. Font-Ribera, E. Gaztanaga, S. G. A. Gontcho, K. Honscheid, J. Jimenez, D. Joyce, R. Kehoe, T. Kisner, A. Kremin, M. Landriau, L. Le Guillou, C. Magneville, P. Martini, R. Miquel, J. Moustakas, J. Nie, W. Percival, C. Poppett, F. Prada, G. Rossi, D. Schlegel, M. Schubnell, H.-J. Seo, R. Sharples, G. Tarle, M. Vargas-Magana, and Z. Zhou, The Optical Corrector for the Dark Energy Spectroscopic Instrument, arXiv e-prints , arXiv:2306.06310 (2023), arXiv:2306.06310 [astro-ph.IM].
- [24] A. B. Pace and L. E. Strigari, Scaling relations for dark matter annihilation and decay profiles in dwarf spheroidal galaxies, *MNRAS* **482**, 3480 (2019), arXiv:1802.06811 [astro-ph.GA].
- [25] J. Guy, S. Bailey, A. Kremin, S. Alam, D. M. Alexander, C. Allende Prieto, S. BenZvi, A. S. Bolton, D. Brooks, E. Chaussidon, A. P. Cooper, K. Dawson, A. de la Macorra, A. Dey, B. Dey, G. Dhungana, D. J. Eisenstein, A. Font-Ribera, J. E. Forero-Romero, E. Gaztañaga, S. Gontcho A Gontcho, D. Green, K. Honscheid, M. Ishak, R. Kehoe, D. Kirkby, T. Kisner, S. E. Koposov, T.-W. Lan, M. Landriau, L. Le Guillou, M. E. Levi, C. Magneville, C. J. Manser, P. Martini, A. M. Meisner, R. Miquel, J. Moustakas, A. D. Myers, J. A. Newman, J. Nie, N. Palanque-Delabrouille, W. J. Percival, C. Poppett, F. Prada, A. Raichoor, C. Ravoux, A. J. Ross, E. F. Schlaflay, D. Schlegel, M. Schubnell, R. M. Sharples, G. Tarlé, B. A. Weaver, C. Yéche, R. Zhou, Z. Zhou, and H. Zou, The Spectroscopic Data Processing Pipeline for the Dark Energy Spectroscopic Instrument, *AJ* **165**, 144 (2023), arXiv:2209.14482 [astro-ph.IM].
- [26] DESI Collaboration, A. G. Adame, J. Aguilar, S. Ahlen, S. Alam, G. Aldering, D. M. Alexander, R. Alfarsy, C. Allende Prieto, M. Alvarez, O. Alves, A. Anand, F. Andrade-Oliveira, E. Armengaud, J. Asorey, S. Avila, A. Aviles, S. Bailey, A. Balaguera-Antolínez, O. Ballester, C. Baltay, A. Bault, J. Bautista, J. Behera, S. F. Beltran, S. BenZvi, L. Beraldo e Silva, J. R. Bermejo-Climent, A. Berti, R. Besuner, F. Beutler, D. Bianchi, C. Blake, R. Blum, A. S. Bolton, S. Brieden, A. Brodzeller, D. Brooks, Z. Brown, E. Buckley-Geer, E. Burtin, L. Cabayol-Garcia, Z. Cai, R. Canning, L. Cardiel-Sas, A. Carnero Rosell, F. J. Castander, J. L. Cervantes-Cota, S. Chabanier, E. Chaussidon, J. Chaves-Montero, S. Chen, C. Chuang, T. Claybaugh, S. Cole, A. P. Cooper, A. Cuceu, T. M. Davis, K. Dawson, R. de Belsunce, R. de la Cruz, A. de la Macorra, A. de Mattia, R. Demina, U. Demirbozan, J. DeRose, A. Dey, B. Dey, G. Dhungana, J. Ding, Z. Ding, P. Doel, R. Doshi, K. Douglass, A. Edge, S. Eftekharzadeh, D. J. Eisenstein, A. Elliott, S. Escoffier, P. Fagrelius, X. Fan, K. Fanning, V. A. Fawcett, S. Ferraro, J. Ereza, B. Flaugher, A. Font-Ribera, D. Forero-Sánchez, J. E. Forero-Romero, C. S. Frenk, B. T. Gänsicke, L. Á. García, J. García-Bellido, C. Garcia-Quintero, L. H. Garrison, H. Gil-Marín, J. Golden-Marx, S. G. A. Gontcho, A. X. Gonzalez-Morales, V. Gonzalez-Perez, C. Gordon, O. Graur, D. Green, D. Gruen, J. Guy, B. Hadzhiyska, C. Hahn, J. J. Han, M. M. S. Hanif, H. K. Herrera-Alcantar, K. Honscheid, J. Hou, C. Howlett, D. Huterer, V. Iršič, M. Ishak, A. Jana, L. Jiang, J. Jimenez, Y. P. Jing, S. Joudaki, E. Jullo, S. Juneau, N. Kizhuprakkat, N. G. Karaçayh, T. Karim, R. Kehoe, S. Kent, A. Khederlarian, S. Kim, D. Kirkby, T. Kisner, F. Kitaura, J. Kneib, S. E. Koposov, A. Kovács, A. Kremin, A. Krolewski, B. L'Huillier, A. Lambert, C. Lamman, T. W. Lan, M. Landriau, D. Lang, J. U. Lange, J. Lasker, L. Le Guillou, A. Leauthaud, M. E. Levi, T. S. Li, E. Linder, A. Lyons, C. Magneville, M. Mancera, C. J. Manser, D. Margala, P. Martini, P. McDonald, G. E. Medina, L. Medina-Varela, A. Meisner, J. Mená Fernández, J. Meneses-Rizo, M. Mezcua, R. Miquel, P. Montero-Camacho, J. Moon, S. Moore, J. Moustakas, E. Mueller, J. Mundet, A. Muñoz-Gutiérrez, A. D. Myers, S. Nadathur, L. Napolitano, R. Neveux, J. A. Newman, J. Nie, G. Niz, P. Norberg, H. E. Noriega, E. Paillas, N. Palanque-Delabrouille, A. Palmese, P. Zhiwei, D. Parkinson, S. Penmetsa, W. J. Percival, A. Pérez-Fernández, I. Pérez-Ràfols, M. Pieri, C. Poppett, A. Porredon, F. Prada, R. Pucha, A. Raichoor, C. Ramírez-Pérez, S. Ramirez-Solano, M. Rashkovetskyi, C. Ravoux, A. Rocher, C. Rockosi, A. J. Ross, G. Rossi, R. Ruggeri, V. Ruhlmann-Kleider, C. G. Sabiu, K. Said, A. Saintonge, L. Samushia, E. Sanchez, C. Saulder, E. Schaan, E. F. Schlaflay, D. Schlegel, D. Scholte, M. Schubnell, H. Seo, A. Shafieloo, R. Sharples, W. Sheu, J. Silber, F. Sinigaglia, M. Siudek, Z. Slepian, A. Smith, D. Sprayberry, L. Stephey, J. Suárez-Pérez, Z. Sun, T. Tan, G. Tarlé, R. Tojeiro, L. A. Ureña-López, R. Vaisakh, D. Valcin, F. Valdes, M. Valluri, M. Vargas-Magaña, A. Variu, L. Verde, M. Walther, B. Wang, M. S. Wang, B. A. Weaver, N. Weaverdyck, R. H. Wechsler, M. White, Y. Xie, J. Yang, C. Yéche, J. Yu, S. Yuan, H. Zhang, Z. Zhang, C. Zhao, Z. Zheng, R. Zhou, Z. Zhou, H. Zou, S. Zou, and Y. Zu, Validation of the Scientific Program for the Dark Energy Spectroscopic Instrument, arXiv e-prints , arXiv:2306.06307 (2023), arXiv:2306.06307 [astro-ph.CO].
- [27] DESI Collaboration, A. G. Adame, J. Aguilar, S. Ahlen, S. Alam, G. Aldering, D. M. Alexander, R. Alfarsy, C. Allende Prieto, M. Alvarez, O. Alves, A. Anand, F. Andrade-Oliveira, E. Armengaud, J. Asorey, S. Avila, A. Aviles, S. Bailey, A. Balaguera-Antolínez, O. Ballester, C. Baltay, A. Bault, J. Bautista, J. Behera, S. F. Beltran, S. BenZvi, L. Beraldo e Silva, J. R. Bermejo-Climent, A. Berti, R. Besuner, F. Beutler, D. Bianchi, C. Blake, R. Blum, A. S. Bolton, S. Brieden, A. Brodzeller, D. Brooks, Z. Brown, E. Buckley-Geer, E. Burtin, L. Cabayol-Garcia, Z. Cai, R. Canning, L. Cardiel-Sas, A. Carnero Rosell, F. J. Castander, J. L. Cervantes-Cota, S. Chabanier, E. Chaussidon, J. Chaves-Montero, S. Chen, C. Chuang, T. Claybaugh, S. Cole, A. P. Cooper, A. Cuceu, T. M. Davis, K. Dawson, R. de Belsunce, R. de la Cruz, A. de la Macorra, A. de Mattia, R. Demina, U. Demirbozan, J. DeRose, A. Dey, B. Dey, G. Dhungana, J. Ding, Z. Ding, P. Doel, R. Doshi, K. Douglass, A. Edge, S. Eftekharzadeh, D. J. Eisenstein, A. Elliott, S. Escoffier, P. Fagrelius, X. Fan, K. Fanning, V. A. Fawcett, S. Ferraro, J. Ereza, B. Flaugher, A. Font-Ribera, D. Forero-Sánchez, J. E. Forero-Romero, C. S. Frenk, B. T. Gänsicke, L. Á. García, J. García-Bellido, C. Garcia-Quintero, L. H. Gar-

- rison, H. Gil-Marín, J. Golden-Marx, S. G. A. Gontcho, A. X. Gonzalez-Morales, V. Gonzalez-Perez, C. Gordon, O. Graur, D. Green, D. Gruen, J. Guy, B. Hadzhiyska, C. Hahn, J. J. Han, M. M. S. Hanif, H. K. Herrera-Alcantar, K. Honscheid, J. Hou, C. Howlett, D. Huterer, V. Iršić, M. Ishak, A. Jacques, A. Jana, L. Jiang, J. Jimenez, Y. P. Jing, S. Joudaki, E. Jullo, S. Juneau, N. Kizhuprakkat, N. G. Karaçaylı, T. Karim, R. Kehoe, S. Kent, A. Khederlarian, S. Kim, D. Kirkby, T. Kisner, F. Kitaura, J. Kneib, S. E. Koposov, A. Kovács, A. Kremin, A. Krolewski, B. L'Huillier, A. Lambert, C. Lamman, T. W. Lan, M. Landriau, D. Lang, J. U. Lange, J. Lasker, L. Le Guillou, A. Leauthaud, M. E. Levi, T. S. Li, E. Linder, A. Lyons, C. Magneville, M. Manera, C. J. Manser, D. Margala, P. Martini, P. McDonald, G. E. Medina, L. Medina-Varela, A. Meissner, J. Mena-Fernández, J. Meneses-Rizo, M. Mezcua, R. Miquel, P. Montero-Camacho, J. Moon, S. Moore, J. Moustakas, E. Mueller, J. Mundet, A. Muñoz-Gutiérrez, A. D. Myers, S. Nadathur, L. Napolitano, R. Neveux, J. A. Newman, J. Nie, R. Nikutta, G. Niz, P. Norberg, H. E. Noriega, E. Paillas, N. Palanque-Delabrouille, A. Palmese, P. Zhiwei, D. Parkinson, S. Penmetsa, W. J. Percival, A. Pérez-Fernández, I. Pérez-Ràfols, M. Pieri, C. Poppett, A. Porredon, S. Pothier, F. Prada, R. Pucha, A. Raichoor, C. Ramírez-Pérez, S. Ramirez-Solano, M. Rashkovetskyi, C. Ravoux, A. Rocher, C. Rockosi, A. J. Ross, G. Rossi, R. Ruggeri, V. Ruhlmann-Kleider, C. G. Sabiu, K. Said, A. Saitonge, L. Samushia, E. Sanchez, C. Saulder, E. Schaan, E. F. Schlafly, D. Schlegel, D. Scholte, M. Schubnell, H. Seo, A. Shafieloo, R. Sharples, W. Sheu, J. Silber, F. Sinigaglia, M. Siudek, Z. Slepian, A. Smith, D. Sprayberry, L. Stephey, J. Suárez-Pérez, Z. Sun, T. Tan, G. Tarlé, R. Tojeiro, L. A. Ureña-López, R. Vaisakh, D. Valcin, F. Valdes, M. Valluri, M. Vargas-Magaña, A. Variu, L. Verde, M. Walther, B. Wang, M. S. Wang, B. A. Weaver, N. Weaverdyck, R. H. Wechsler, M. White, Y. Xie, J. Yang, C. Yèche, J. Yu, S. Yuan, H. Zhang, Z. Zhang, C. Zhao, Z. Zheng, R. Zhou, Z. Zhou, H. Zou, S. Zou, and Y. Zu, The Early Data Release of the Dark Energy Spectroscopic Instrument, arXiv e-prints , arXiv:2306.06308 (2023), arXiv:2306.06308 [astro-ph.CO].
- [28] C. Hahn, M. J. Wilson, O. Ruiz-Macias, S. Cole, D. H. Weinberg, J. Moustakas, A. Kremin, J. L. Tinker, A. Smith, R. H. Wechsler, S. Ahlen, S. Alam, S. Bailey, D. Brooks, A. P. Cooper, T. M. Davis, K. Dawson, A. Dey, B. Dey, S. Eftekharzadeh, D. J. Eisenstein, K. Fanning, J. E. Forero-Romero, C. S. Frenk, E. Gaztañaga, S. Gontcho A Gontcho, J. Guy, K. Honscheid, M. Ishak, S. Juneau, R. Kehoe, T. Kisner, T.-W. Lan, M. Landriau, L. Le Guillou, M. E. Levi, C. Magneville, P. Martini, A. Meissner, A. D. Myers, J. Nie, P. Norberg, N. Palanque-Delabrouille, W. J. Percival, C. Poppett, F. Prada, A. Raichoor, A. J. Ross, S. Safonova, C. Saulder, E. Schlafly, D. Schlegel, D. Sierra-Porta, G. Tarle, B. A. Weaver, C. Yèche, P. Zarrouk, R. Zhou, Z. Zhou, and H. Zou, The DESI Bright Galaxy Survey: Final Target Selection, Design, and Validation, *AJ* **165**, 253 (2023), arXiv:2208.08512 [astro-ph.CO].
- [29] A. Dey, D. J. Schlegel, D. Lang, R. Blum, K. Burleigh, X. Fan, J. R. Findlay, D. Finkbeiner, D. Herrera, S. Juneau, M. Landriau, M. Levi, I. McGreer, A. Meissner, A. D. Myers, J. Moustakas, P. Nugent, A. Patej, E. F. Schlafly, A. R. Walker, F. Valdes, B. A. Weaver, C. Yèche, H. Zou, X. Zhou, B. Abareshi, T. M. C. Abbott, B. Abolfathi, C. Aguilera, S. Alam, L. Allen, A. Alvarez, J. Annis, B. Ansarinejad, M. Aubert, J. Beechert, E. F. Bell, S. Y. BenZvi, F. Beutler, R. M. Bielby, A. S. Bolton, C. Briceño, E. J. Buckley-Geer, K. Butler, A. Calamida, R. G. Carlberg, P. Carter, R. Casas, F. J. Castander, Y. Choi, J. Comparat, E. Cukanovaite, T. Delubac, K. DeVries, S. Dey, G. Dhungana, M. Dickinson, Z. Ding, J. B. Donaldson, Y. Duan, C. J. Duckworth, S. Eftekharzadeh, D. J. Eisenstein, T. Etourneau, P. A. Fagrelius, J. Farihi, M. Fitzpatrick, A. Font-Ribera, L. Fulmer, B. T. Gänsicke, E. Gaztanaga, K. George, D. W. Gerdes, S. G. A. Gontcho, C. Gorgoni, G. Green, J. Guy, D. Harmer, M. Hernandez, K. Honscheid, L. W. Huang, D. J. James, B. T. Jannuzzi, L. Jiang, R. Joyce, A. Karcher, S. Karkar, R. Kehoe, J.-P. Kneib, A. Kueter-Young, T.-W. Lan, T. R. Lauer, L. Le Guillou, A. Le Van Suu, J. H. Lee, M. Lesser, L. Perreault Levasseur, T. S. Li, J. L. Mann, R. Marshall, C. E. Martínez-Vázquez, P. Martini, H. du Mas des Bourboux, S. Manus, T. G. Meier, B. Ménard, N. Metcalfe, A. Muñoz-Gutiérrez, J. Najita, K. Napier, G. Narayan, J. A. Newman, J. Nie, B. Nord, D. J. Norman, K. A. G. Olsen, A. Paat, N. Palanque-Delabrouille, X. Peng, C. L. Poppett, M. R. Poremba, A. Prakash, D. Rabinowitz, A. Raichoor, M. Rezaie, A. N. Robertson, N. A. Roe, A. J. Ross, N. P. Ross, G. Rudnick, S. Safonova, A. Saha, F. J. Sánchez, E. Savary, H. Schweiker, A. Scott, H.-J. Seo, H. Shan, D. R. Silva, Z. Slepian, C. Soto, D. Sprayberry, R. Staten, C. M. Stillman, R. J. Stupak, D. L. Summers, S. Sien Tie, H. Tirado, M. Vargas-Magaña, A. K. Vivas, R. H. Wechsler, D. Williams, J. Yang, Q. Yang, T. Yapici, D. Zaritsky, A. Zenteno, K. Zhang, T. Zhang, R. Zhou, and Z. Zhou, Overview of the DESI Legacy Imaging Surveys, *AJ* **157**, 168 (2019), arXiv:1804.08657 [astro-ph.IM].
- [30] H. Zou, X. Zhou, X. Fan, T. Zhang, Z. Zhou, J. Nie, X. Peng, I. McGreer, L. Jiang, A. Dey, D. Fan, B. He, Z. Jiang, D. Lang, M. Lesser, J. Ma, S. Mao, D. Schlegel, and J. Wang, Project Overview of the Beijing-Arizona Sky Survey, *PASP* **129**, 064101 (2017), arXiv:1702.03653 [astro-ph.GA].
- [31] R. Zhou, B. Dey, J. A. Newman, D. J. Eisenstein, K. Dawson, S. Bailey, A. Berti, J. Guy, T.-W. Lan, H. Zou, J. Aguilar, S. Ahlen, S. Alam, D. Brooks, A. de la Macorra, A. Dey, G. Dhungana, K. Fanning, A. Font-Ribera, S. G. A. Gontcho, K. Honscheid, M. Ishak, T. Kisner, A. Kovács, A. Kremin, M. Landriau, M. E. Levi, C. Magneville, M. Manera, P. Martini, A. M. Meissner, R. Miquel, J. Moustakas, A. D. Myers, J. Nie, N. Palanque-Delabrouille, W. J. Percival, C. Poppett, F. Prada, A. Raichoor, A. J. Ross, E. Schlafly, D. Schlegel, M. Schubnell, G. Tarlé, B. A. Weaver, R. H. Wechsler, C. Yèche, and Z. Zhou, Target Selection and Validation of DESI Luminous Red Galaxies, *AJ* **165**, 58 (2023), arXiv:2208.08515 [astro-ph.CO].
- [32] A. D. Myers, J. Moustakas, S. Bailey, B. A. Weaver, A. P. Cooper, J. E. Forero-Romero, B. Abolfathi, D. M. Alexander, D. Brooks, E. Chaussidon, C.-H. Chuang, K. Dawson, A. Dey, B. Dey, G. Dhungana, P. Doel, K. Fanning, E. Gaztañaga, S. Gontcho A Gontcho, A. X. Gonzalez-Morales, C. Hahn, H. K. Herrera-Alcantar,

- K. Honscheid, M. Ishak, T. Karim, D. Kirkby, T. Kisner, S. E. Koposov, A. Kremin, T.-W. Lan, M. Landriau, D. Lang, M. E. Levi, C. Magneville, L. Napolitano, P. Martini, A. Meisner, J. A. Newman, N. Palanque-Delabrouille, W. Percival, C. Poppett, F. Prada, A. Raichoor, A. J. Ross, E. F. Schlafly, D. Schlegel, M. Schubnell, T. Tan, G. Tarle, M. J. Wilson, C. Yèche, R. Zhou, Z. Zhou, and H. Zou, The Target-selection Pipeline for the Dark Energy Spectroscopic Instrument, *AJ* **165**, 50 (2023), arXiv:2208.08518 [astro-ph.IM].
- [33] P. Virtanen, R. Gommers, T. E. Oliphant, M. Haberland, T. Reddy, D. Cournapeau, E. Burovski, P. Peterson, W. Weckesser, J. Bright, S. J. van der Walt, M. Brett, J. Wilson, K. J. Millman, N. Mayorov, A. R. J. Nelson, E. Jones, R. Kern, E. Larson, C. J. Carey, I. Polat, Y. Feng, E. W. Moore, J. VanderPlas, D. Laxalde, J. Perktold, R. Cimrman, I. Henriksen, E. A. Quintero, C. R. Harris, A. M. Archibald, A. H. Ribeiro, F. Pedregosa, P. van Mulbregt, and SciPy 1.0 Contributors, SciPy 1.0: Fundamental Algorithms for Scientific Computing in Python, *Nature Methods* **17**, 261 (2020).
- [34] O. Ruiz-Macias, P. Zarrouk, S. Cole, P. Norberg, C. Baugh, D. Brooks, A. Dey, Y. Duan, S. Eftekharzadeh, D. J. Eisenstein, J. E. Forero-Romero, E. Gaztañaga, C. Hahn, R. Kehoe, M. Landriau, D. Lang, M. E. Levi, J. Lucey, A. M. Meisner, J. Moustakas, A. D. Myers, N. Palanque-Delabrouille, C. Poppett, F. Prada, A. Raichoor, D. J. Schlegel, M. Schubnell, G. Tarlé, D. H. Weinberg, M. J. Wilson, and C. Yèche, Preliminary Target Selection for the DESI Bright Galaxy Survey (BGS), *Research Notes of the American Astronomical Society* **4**, 187 (2020), arXiv:2010.11283 [astro-ph.GA].
- [35] G. D. Illingworth, D. Magee, P. A. Oesch, R. J. Bouwens, I. Labb  , M. Stiavelli, P. G. van Dokkum, M. Franx, M. Trenti, C. M. Carollo, and V. Gonzalez, The HST eXtreme Deep Field (XDF): Combining All ACS and WFC3/IR Data on the HUDF Region into the Deepest Field Ever, *ApJS* **209**, 6 (2013), arXiv:1305.1931 [astro-ph.CO].
- [36] P. Fischer, T. A. McKay, E. Sheldon, A. Connolly, A. Stebbins, J. A. Frieman, B. Jain, M. Joffre, D. Johnston, G. Bernstein, J. Annis, N. A. Bahcall, J. Brinkmann, M. A. Carr, I. Csabai, J. E. Gunn, G. S. Hennessy, R. B. Hindsley, C. Hull,   . Ivezi  , G. R. Knapp, S. Limmongkol, R. H. Lupton, J. A. Munn, T. Nash, H. J. Newberg, R. Owen, J. R. Pier, C. M. Rockosi, D. P. Schneider, J. A. Smith, C. Stoughton, A. S. Szalay, G. P. Szokoly, A. R. Thakar, M. S. Vo geley, P. Waddell, D. H. Weinberg, D. G. York, and SDSS Collaboration, Weak Lensing with Sloan Digital Sky Survey Commissioning Data: The Galaxy-Mass Correlation Function to 1 H^{-1} Mpc, *AJ* **120**, 1198 (2000), arXiv:astro-ph/9912119 [astro-ph].
- [37] E. S. Sheldon, D. E. Johnston, J. A. Frieman, R. Scerri-ton, T. A. McKay, A. J. Connolly, T. Budav  i, I. Zehavi, N. A. Bahcall, J. Brinkmann, and M. Fukugita, The Galaxy-Mass Correlation Function Measured from Weak Lensing in the Sloan Digital Sky Survey, *AJ* **127**, 2544 (2004), arXiv:astro-ph/0312036 [astro-ph].
- [38] X. Xu and E. R. Siegel, Dark Matter in the Solar System, arXiv e-prints , arXiv:0806.3767 (2008), arXiv:0806.3767 [astro-ph].
- [39] R. A. Bernstein, The optical extragalactic background light: Revisions and further comments, *The Astrophysical Journal* **666**, 663 (2007).
- [40] T. R. Lauer, M. Postman, H. A. Weaver, J. R. Spencer, S. A. Stern, M. W. Buie, D. D. Durda, C. M. Lisse, A. R. Poppe, R. P. Binzel, D. T. Britt, B. J. Buratti, A. F. Cheng, W. M. Grundy, M. Hor  nyi, J. J. Kavelaars, I. R. Linscott, W. B. McKinnon, J. M. Moore, J. I. N  nez, C. B. Olkin, J. W. Parker, S. B. Porter, D. C. Reuter, S. J. Robbins, P. Schenk, M. R. Showalter, K. N. Singer, A. J. Verbiscer, and L. A. Young, New Horizons Observations of the Cosmic Optical Background, *ApJ* **906**, 77 (2021), arXiv:2011.03052 [astro-ph.GA].
- [41] T. R. Lauer, M. Postman, J. R. Spencer, H. A. Weaver, S. A. Stern, G. R. Gladstone, R. P. Binzel, D. T. Britt, M. W. Buie, B. J. Buratti, A. F. Cheng, W. M. Grundy, M. Hor  nyi, J. J. Kavelaars, I. R. Linscott, C. M. Lisse, W. B. McKinnon, R. L. McNutt, J. M. Moore, J. I. N  nez, C. B. Olkin, J. W. Parker, S. B. Porter, D. C. Reuter, S. J. Robbins, P. M. Schenk, M. R. Showalter, K. N. Singer, A. J. Verbiscer, and L. A. Young, Anomalous Flux in the Cosmic Optical Background Detected with New Horizons Observations, *ApJ* **927**, L8 (2022), arXiv:2202.04273 [astro-ph.GA].
- [42] C. Creque-Sarbinowski and M. Kamionkowski, Searching for decaying and annihilating dark matter with line intensity mapping, *Phys. Rev. D* **98**, 063524 (2018), arXiv:1806.11119 [astro-ph.CO].
- [43] J. L. Bernal, A. Caputo, and M. Kamionkowski, Strategies to detect dark-matter decays with line-intensity mapping, *Phys. Rev. D* **103**, 063523 (2021), arXiv:2012.00771 [astro-ph.CO].
- [44] J. L. Bernal, G. Sato-Polito, and M. Kamionkowski, The cosmic optical background excess, dark matter, and line-intensity mapping, arXiv e-prints , arXiv:2203.11236 (2022), arXiv:2203.11236 [astro-ph.CO].